KINETICS OF 1-PENTANOL ETHERIFICATION WITHOUT WATER REMOVAL

Roger Bringué, Eliana Ramírez, Carles Fité, Montserrat Iborra and Javier Tejero*

*Dept. of Chemical Engineering, University of Barcelona. C/ Martí i Franquès, 1, 08028-Barcelona, SPAIN *Corresponding author*: Phone: +34 93 4020155; Fax: +34 93 4021291; E-mail: rogerbringue@ub.edu

Abstract

The effect of water on the kinetics of the liquid-phase dehydration of 1-pentanol to di-*n*-pentyl ether (DNPE) and water over Amberlyst 70 is revisited. To explain the strong inhibitor effect of water, two approaches were compared. Firstly, a model stemming from a Langmuir- Hinshelwood-Hougen-Watson (LHHW) mechanism was used, wherein the inhibitor effect of water was explained by the competitive adsorption of water and pentanol. Secondly, a modified Eley-Rideal (ER) model that includes an inhibition factor, in which a Freundlich-like function is used to explain the inhibitor effect of water by blocking the access of pentanol to the active centers. Both models fitted data quite well, although the best results were obtained with the modified ER model. The activation energy was 118.7 ± 0.2 kJ/mol for the LHHW model and 114.0 ± 0.1 kJ/mol for the modified ER one.

Keywords: inhibiting effect of water, 1-pentanol, DNPE, Amberlyst 70, Reaction kinetics

1. Introduction

Adsorption of chemicals on the solid surface is the key step of solid catalyzed reactions, so that interaction among one or more of the different species present in the medium with

catalyst surface is essential for the reaction to proceed. Frequently, some reactant or reaction product adsorbs preferably determining in this way the catalyst activity, i.e. polar species onto sulfonic styrene/divinylbenzene (S/DVB) resins. In such catalysts acidity and accessibility of sulfonic groups to catalyze the reaction change over reaction medium composition because of polymer swelling by the preferential adsorption of species such as water or alcohol what decreases, as a result, the reaction rate[1].

This rate-inhibiting effect of polar species on S/DVB resins is advantageously used to maximize the yield of the intermediate product in series reactions by limiting the yield of final products, e.g. alcohols[2,3] and water[4,5] are reported as selectivity enhancers in olefin oligomerization, favoring dimers formation and hindering that of trimers and higher oligomers. More often, this effect is undesirable when such polar species, in particular water, are reaction products. As a highly polar species, it preferably adsorbs on sulfonic S/DVB resins with a rate-inhibiting effect both in gas phase[6] and in liquid phase reactions[7-19]. Kinetics of liquid-phase reactions with water formation (alcohol dehydration to olefins, bisphenol A synthesis, etc) is complex since the very first amount of water produced inhibits the reaction, whereas further water released acts as a solvent[7], what swells the resin and increases accessibility to inner active centers. This process is accompanied simultaneously by a transition from general to specific acid catalysis, generally slower[7]. The rate-inhibiting effect of water is also ascribed to its great affinity for sulfonic groups, so that it excludes the reactants and suppresses the catalytic reaction almost completely[20,21]. However, it is to be noted that, despite its rate-inhibiting effect, water is reported to improve the catalyst's lifetime[16].

Langmuir-Hinshelwood-Hougen-Watson (LHHW) or its related Eley-Rideal (ER) kinetic models are widely used to represent rate data of liquid-phase reactions of alcohol

dehydration to ether[10,22-24], but some inaccuracies appear because of the reaction medium-catalyst interaction, specially on catalysts with a flexible backbone as S/DVB resins. To quantify the effect of such interaction, empirical corrections are suggested in the open literature. Water effect has been represented by using empirical exponents in the driving force and the adsorption term of LHHW or ER rate-expressions, i.e. for tert-butanol dehydration[7], esterification of acetic acid with amyl alcohol[12] or synthesis of tertiary amyl alcohol[25]. In the particular case of liquid-phase etherification reactions, a second approach is found: water effect on the reaction rate is quantified by splitting off the rate constant, $\hat{k}$, into two factors as a product of the true rate constant, $\hat{k}_o$, and an inhibition factor, which should take values between 0 and 1 and depends on temperature and water activity, a_w, in the liquid-phase. Such factor is analogous to those mostly used to describe catalyst deactivation by poisoning and, at first sight, it can be seen as the fraction of active centers free of water[17-19], $(1-\theta_w)$, i.e.,

$$\hat{k} = \hat{k}_o \cdot f\left(a_w, T\right) = \hat{k}_o\left(1-\theta_w\right) \qquad (1)$$

In a previous work, the liquid phase dehydration of 1-pentanol to DNPE without water removal was studied on gel and macroporous acidic S/DVB resins, including sulfonated and over-sulfonated ones[26,27]. Gel-type and low-crosslinking macroporous resins were found to be very selective to DNPE and, therefore, they are suitable catalysts for the reaction. Among tested resins, the thermally stable Amberlyst 70, which is able to operate up to 463 K, was proposed for industrial use, since it showed the highest conversion and yield in the temperature range 423-463 K. Its performance in this temperature range was even better than Nafion NR50 or H-Beta zeolite.

In a first approach to obtain the reaction kinetics, necessary for reactor design purposes, it was found that a kinetic model based on an ER mechanism, in which the rate-limiting step was the surface reaction between adsorbed 1-pentanol and an alcohol molecule from the liquid phase and without a significant number of unoccupied active centers, represented reasonably well rate data for all the tested catalysts[27]:

$$r_{DNPE} = \frac{\hat{k} \cdot a_P^2}{a_P + \left(K_D / K_p \right) \cdot a_D} \qquad (2)$$

K_D and K_P are the adsorption equilibrium constants of DNPE and 1-pentanol; a_D and a_p, their liquid-phase activities, respectively, and $\hat{k}$ the rate constant. However, at 453 and 463 K some inaccuracies were noted in the case of Amberlyst 70. As a consequence the rate model should be upgraded, by considering (a) the reverse reaction and (b) the effect of water in the reaction rate, seeing that water activity does not accounts in eq.(2), despite the fact that water adsorbs in large amounts in ion-exchange resins.

Lately, equilibrium constants for the liquid-phase dehydration of 1-pentanol to DNPE were determined experimentally[28]. Moreover, the inhibiting effect of water on the rate of the liquid-phase dehydration of 1-pentanol to DNPE was stated experimentally and some kinetic models including water effect were proposed[29]. A complete and exhaustive kinetic study of the reaction including the last findings on the reaction is thus suitable. As a consequence, the aim of this work is to perform a comprehensive kinetic analysis of DNPE synthesis on Amberlyst 70 by including both (a) the effect of the reverse reaction and (b) new rate data obtained in the presence of additional water and ether amounts, in such a way that it was possible to discriminate a good kinetic model able to predict reaction rate in a wide range of alcohol, ether and water concentrations.

2. Experimental

2.1 Materials

1-Pentanol (99% pure, <1% 2-methyl-1-butanol), supplied by Fluka, and bidistilled water were used without further purification. DNPE (≥ 99 %) was produced and purified in our laboratory. Amberlyst 70 (Rohm & Haas), a macroporous sulfonic styrene-DVB resin stable up to 473K (surface area 29.9 m^2/g when dried by successive percolation with methanol, toluene and isooctane; concentration of acid sites 3 eq H^+/kg) was used as the catalyst.

2.2 Apparatus

Experiments were carried out in a 100 mL stainless steel autoclave operated in batch mode. A magnetic drive turbine was used as stirring device and baffles were placed inside the reactor to improve mixing. Temperature was controlled to within ±1 K by an electric furnace. The pressure was set at 1.6 MPa by means of N_2, in order to maintain the liquid phase over the whole temperature range. One of the outlets was connected directly to a liquid sampling valve, which injected 0.2 μL of liquid into a GLC chromatograph.

2.3 Analysis

The liquid composition was analyzed by a split operation mode in a HP6890A GLC apparatus equipped with a TCD detector. A 50m × 0.2mm × 0.5 μm methyl silicone capillary column was used to quantify concentration of 1-pentanol, DNPE, water, 1-pentene, 2-pentene, and branched ethers 1-(1-methyl-butoxy)-pentane, 1-(2-methyl-butoxy)-pentane, 2-(1-methyl-butoxy)-pentane, and 2-(2-methyl-butoxy)-pentane. The temperature of the column was held at 318 K for 6 min, increased at a rate of 30 K/min up

to 453 K, and held for 2 min. Helium was used as carrier gas at a total flow rate of 30 mL/min.

2.3 Procedure

Fresh catalyst and 70 mL of 1-pentanol (1-pentanol-water or 1-pentanol-DNPE where appropriate) were charged into the reactor and, after checking for leakages, heated to the working temperature. The resin was dried for 1 h in atmospheric oven at 383K, and then for 2 h at vacuum (< 0.1 mmHg). Zero time was set when the reaction medium reached working temperature. To monitor the concentration variation of chemicals along time, very small liquid samples, which do not disturb the reacting system, were taken out of the reactor and analyzed hourly. Reaction rates of DNPE formation were estimated as indicated elsewhere[27], being accurate within ± 5%. On the other hand, in all the experiments mass balance was fulfilled within ± 2 %.

3. Results and discussion

3.1. Preliminary experiments

Firstly preliminary runs were conducted at 463 K to check that measured rates were free of mass transfer effects. All the experiments were performed on 1 g of catalyst, since previous results with the same set-up showed that with a catalyst mass ≤ 2 g, measured rates were independent on the amount of used catalyst[27,30].

Diffusion rate of chemicals through porous solids depends on temperature and particle size. To measure intrinsic reaction rates experimentally, and so have an accurate kinetic model, it is basic to work within the particle diameter, d_p, range where such influence is negligible. Internal mass transfer influence can be evaluated by testing catalyst batches of different particle size. Figure 1 (up) plots DNPE mole profile along time for different

particle size batches, whereas in Figure 1 (down) the initial reaction rate at 463 K is plotted against the reciprocal of resin mean particle diameter. Open circles correspond to Amberlyst 70 sieved fractions of 0.316, 0.502, 0.710 and > 0.8 mm, respectively, and the black rhombus refers to the mean diameter of commercial beads (0.570 mm). As Figure 1 (up) shows, internal mass transfer influence is negligible at 463K within the limits of the experimental error in the particle size range explored, and therefore also at lower temperatures, although the DNPE mole profile for d_p = 0.7 mm is slightly higher than the others after 6 h. This fact is ascribed to the accumulation of the experimental error throughout the whole experiment, since no deviation was observed on the commercial distribution of particle diameters.

External mass transfer influence was evaluated by performing a series of experiments by changing stirring speed, *N*, between 50 and 700 rpm, also at 463K, where such influence could be more notorious. In Figure 2 DNPE mole evolution versus time at different stirring speeds and the initial reaction rate versus stirring speed are shown. As can be seen, initial reaction rates are the same, within the limits of experimental error, for N ≥ 200 rpm, whereas DNPE mole profiles overlap except when N = 700 and 50 rpm.

As a consequence, to measure intrinsic reaction rates of DNPE synthesis henceforth, experiments were performed at N = 500 rpm on catalyst samples of 1 g of dry catalyst having the commercial distribution of particle sizes.

3.2. Experiments starting with pure 1-pentanol

A first series of replicated experiments were done in the temperature range 413 – 463K starting from pure 1-pentanol[27]. Figure 3 shows DNPE production along the runs. As expected, reaction rate is highly dependent on temperature. The slope of n_{DNPE} vs. time, which is related to reaction rate, diminishes along time due to the effect of the reverse

reaction and/or some inhibition effect. In all the runs, selectivity to ether was higher than 93%.

As the reaction mixture is non-ideal, kinetic analysis is given in terms of activities of 1-pentanol (a_P), DNPE (a_D), and water (a_W). Activity coefficients were computed by the UNIFAC-DORTMUND predictive method[31]. The dependence of the reaction rate as a function of a_P, a_D and a_W is shown in Figure 4. As seen, reaction rate increases on increasing a_P in the entire range of explored activities and temperatures, whereas it decreases on increasing a_D and a_W. These facts suggest that a hyperbolic model, based on a LHHW or ER mechanism, could explain satisfactorily rate data. Figure 4 (up) suggests that a_P influences chiefly the numerator of such a kinetic model, so promoting forward reaction. The rate-decreasing effect showed by a_D and a_W (Figures 4 (middle and down)) can be attributed to a preferential adsorption onto the resin of the ether and water, and also, as they are reaction products, to the enhancement of the reverse reaction as the system approaches to chemical equilibrium[32-33]. Based on the analysis of the reaction rate dependence, and considering the adsorption-reaction–desorption process, the following reaction mechanisms could be proposed:

<u>Mechanism 1</u>: two 1-pentanol molecules adsorbed on an active site, respectively, react to give the ether and water (LHHW type)

$$\text{1-PeOH} + \sigma \rightleftharpoons \text{1-PeOH}\cdot\sigma$$

$$2\,(\text{1-PeOH}\cdot\sigma) \rightleftharpoons \text{DNPE}\cdot\sigma + \text{W}\cdot\sigma$$

$$\text{DNPE}\cdot\sigma \rightleftharpoons \text{DNPE} + \sigma$$

$$\text{W}\cdot\sigma \rightleftharpoons \text{W} + \sigma$$

Mechanism 2: 1-pentanol from solution reacts with 1-pentanol adsorbed on one active centre to give the ether adsorbed on the resin surface, the water being released instantaneously to the liquid phase (ER type)

1-PeOH + σ ⇌ 1-PeOH·σ

1-PeOH·σ + 1-PeOH ⇌ DNPE·σ + W

DNPE·σ ⇌ DNPE + σ

Mechanism 3: 1-pentanol from solution reacts with 1-pentanol adsorbed on one active site, the ether being released directly to the liquid phase (ER type),

1-PeOH + σ ⇌ 1-PeOH·σ

1-PeOH·σ + 1-PeOH ⇌ W·σ + DNPE

W·σ ⇌ W + σ

By assuming that surface reaction is the rate-limiting step, the following kinetic models were obtained for mechanisms 1, 2 and 3, respectively:

$$r_{DNPE} = \frac{\hat{k} \cdot K_P^2 \left(a_P^2 - \frac{a_W a_D}{K} \right)}{\left(1 + K_P a_P + K_D a_D + K_W a_W\right)^2} \tag{3}$$

$$r_{DNPE} = \frac{\hat{k} \cdot K_P \left(a_P^2 - \frac{a_W a_D}{K} \right)}{1 + K_P a_P + K_D a_D} \tag{4}$$

$$r_{DNPE} = \frac{\hat{k} \cdot K_P \left(a_P^2 - \frac{a_W a_D}{K} \right)}{1 + K_P a_P + K_W a_W} \tag{5}$$

On the basis of these equations, all possible kinetic models derived by considering one or more factors of adsorption term being negligible were fitted to rate data. A detailed schedule of models handled can be found elsewhere[34,35]. For fitting purposes, all the models

203 were grouped into two classes, depending on the number of free active centers (see Table
204 1):
205 (i) Class I, for which the number of free active centers is considered to be negligible
206 compared to occupied ones. This fact implies that the unity present in the adsorption term is
207 removed.
208 (ii) Class II, where that hypothesis is rejected.
209 For models of Class I, the surface rate constant, $\hat{k}$, and the adsorption equilibrium
210 constants, K_P, K_D, and K_W, have been grouped into factors, called A, B, and C, for
211 mathematical fitting purposes. The particular form how constants are grouped depends on
212 the mechanism (LHHW or ER) and the neglected adsorption term, if any. Concerning the
213 models of class II, k_1 is equal to $\hat{k}K_P^2$ for LHHW models and to $\hat{k}K_P$ for ER models. The
214 temperature dependence of such factors was defined as follows:

215 $$A, B, C, k_1 = \exp(b_i)\exp\left[-b_{i+1}\left(\frac{1}{T} - \frac{1}{\overline{T}}\right)\right] \quad (6)$$

216 where $\overline{T}$ is the mean experimental temperature. To take into account the influence of the
217 reverse reaction, the temperature dependence of the thermodynamic equilibrium constant,
218 K, was computed as[28]

219 $$K = \exp\left(\frac{783.42}{T} + 2.18\right) \quad (7)$$

220 Fitted parameters of the models shown in Table 1 were b's, as appeared in Equation 6.
221 The subtraction of the inverse of the mean experimental temperature was included to
222 minimize the correlation among fitted parameters b_i and b_{i+1}.
223 From a mathematical point of view, the most suitable model is the one in which the
224 minimum sum of squared residuals (*SSR*), residuals randomness, and lower parameter

correlation is obtained with the minimum number of fitted parameters. On the other hand, these parameters should have a physicochemical meaning, i.e. rate constant, and adsorption equilibrium constants, must increase, and decrease, respectively, with temperature, because reaction activation energy is positive and adsorption enthalpies negative.

Figure 5 shows the goodness of fit in terms of SSR_{min}/SSR, where SSR_{min} is the minimum value obtained for the different models. Obviously, the model with $SSR_{min}/SSR = 1$ is the one with the minimum *SSR*, i.e. the best mathematical fit, while SSR_{min}/SSR tends to zero for worse fits. Models Class II type 4 (from now coded as II-4) with n = 1, II-5 (n = 1, and 2), II-6 (n = 2), and II-7 (n = 2) did not converge or led to results without physicochemical meaning during the fitting procedure. As seen in Figure 5, there are several candidate models using the mathematical criterion of minimum *SSR*, since they led to similar results. Models II-3 (n = 2) and I-7 (n = 2) were the best ones, but I-5 (n =1 and 2), II-3 (n=1), II-4 (n = 2), and II-6 (n=1) were very close. The main characteristic of all these models stems in the adsorption term. In all these models, but II-4 (n=2), a_w participates in the denominator, so the influence of water on the reaction rate seems very clear despite they were not much sensitive to species contribution to the adsorption term, probably because composition of liquid phase was linked by the reaction stoichiometry, at least up to a point.

Figure 6 shows Amberlyst 70 bead size distribution (Beckman Coulter LS Particle Size Analyzer). As seen, particle size distributions in air and DNPE are alike, but resin beads swell about an 8% in 1-pentanol and a 35% in water. Therefore, DNPE hardly adsorbs onto the resin, but it retains 0.16 mol of 1-pentanol per $–SO_3H$ group (computed from data shown in Figure 6) when it is completely swollen in alcohol, and 4.2 mol of H_2O per $–SO_3H$ group when swollen in water. Such water amount agrees with the 3.5-3.85 mol of H_2O per $–SO_3H$ group adsorbed when resins are in equilibrium with atmospheric air at

298K[36]. As adsorption is exothermic, in the working temperature range of Amberlyst 70, which is above 298K, it retains a smaller water amount, but it is enough to swell the resin and to enable the reaction to proceed. Accordingly, it can be assumed that, at first, alcohol penetrates up to some extent in the catalyst and reacts. Released water adsorbs preferentially onto the resin and it swells, enabling diffusion of 1-pentanol and DNPE within the catalyst. Subsequently, when there is some water in the reaction system, it inhibits the reaction, as seen in Figure 4. In his turn, this fact could explain the very slow reaction rates observed when wet catalyst is used instead a dry one. It is to be noted that only models I-5 (n=1 and n=2) are in agreement with these observations, since the others include either the ether in the adsorption term or exclude 1-pentanol.

3.3. Experiments with 1-pentanol/water and 1-pentanol/DNPE mixtures

To stress the effect of water and DNPE on the reaction rate, a set of experiments with 1-pentanol/water and 1-pentanol/DNPE mixtures were performed at 433 and 453 K. Figure 7 plots n_{DNPE} profiles along time of these experiments at 433K. The amount of DNPE produced decreased dramatically on increasing the initial amount of water, as shown in Figure 7 (up), whereas it was hardly affected when initial amounts of DNPE were added (Figure 7 (down)). The same behavior was observed at 453K.

Figure 8 shows the effect of DNPE and water activities on the reaction rate as a function of the initial w/w % of DNPE or water in the mixture. As Figure 8 (up) shows, the effect of DNPE on initial reaction rates is not remarkable. So, the weight of a_D in the adsorption term seems to be negligible. Thereafter, as reaction proceeds, the rate decreases continuously on increasing a_D, and the rate-decreasing effect would be due to the progress of reverse reaction. On the other hand, initial reaction rates are highly sensitive to water content showing clearly its inhibiting effect (Figure 8 (down)). It is to be noted that for $a_W \geq$

273 0.25 reaction rate decreases very slowly, similarly to MTBE synthesis in a large methanol
274 excess[37]. This behavior could be explained by the fact that, at such water levels, reaction
275 proceeds by a specific acid catalytic mechanism, much slower than a general one[7].

276 Models of Table 1 were fitted to the pool of experiments series done with 1-pentanol, 1-
277 pentanol/water and 1-pentanol/DNPE mixtures. Figure 9 shows the goodness of fit in terms
278 of SSR_{min}/SSR. As seen, models I-5 (n = 2) and I-7 (n = 2) yielded the minimum *SSR*.
279 However, fitted values of factor *B* in model I-7 (n = 2) led such factor to value zero in the
280 whole temperature range. So, the term $B \cdot a_D$ was removed from model I-7 (n = 2) becoming
281 in this way the model I-5 (n = 2). Then, the best kinetic model was,

282 $$r_{DNPE} = \frac{A \cdot \left(a_P^2 - \frac{a_w a_D}{K} \right)}{\left(a_P + B \cdot a_W \right)^2} \quad (8)$$

283 By introducing water and DNPE in the initial mixture, a wider concentration and relative
284 proportion ranges between species are achieved. This point, together with the fact that a_W
285 and a_D ranges were large enough, allows us to find a rate model useful in a large reactant
286 and product concentration range, unlike Equation 2 that only described satisfactorily the
287 experimental results for low 1-pentanol conversions and for very small a_W range, where
288 influence of reverse reaction could be neglected. As a consequence, conclusions about the
289 influence of water and DNPE could be ambiguous. Equation 8 stems from the LHHW
290 mechanism (mechanism 1), assuming that DNPE adsorption and the fraction of free active
291 sites are negligible. The noticeable effect of water on the reaction rate is mainly due to its
292 competitive adsorption with 1-pentanol. Equation 8 represents satisfactorily rate data as a
293 whole, however some deviations are observed particularly when there is a large amount of

water in the system i.e. low reaction rates (Figure 10 up). Furthermore, the residual plot shown in Figure 11 (up) is clearly biased.

3.4. Approach by considering blocking of –SO_3H groups by water

A new approach was undertaken following the insight outlined by du Toit and Nicol[19]: released water adsorbs strongly on acidic sites, it hinders 1-pentanol adsorption, and the reaction rate drops. As for LHHW or ER models, the rate constant, $\hat{k}$, is a function of the total amount of available sites. Water effect was modeled, similarly to Eq. 1, by splitting $\hat{k}$ into a "true" rate constant, $\hat{k}_o$, and a function of the fraction of sites free of water (1 - θ_W) which depends on a_W and temperature. Analogously to du Toit and Nicol's work, a Freundlich adsorption isotherm was used to consider the amount of adsorbed water, where n are the sites taking part in the rate-limiting step.

$$\hat{k} = \hat{k}_o \cdot f\left(a_W, T\right) = \hat{k}_o \left(1 - K_W a_W^{1/\alpha}\right)^n \tag{9}$$

$$\text{where } \alpha = \frac{K_\alpha}{T} \tag{10}$$

$$\text{and } K_W = \frac{K_{W1}}{T} \exp\left[-K_{W2}\left(\frac{1}{T} - \frac{1}{\overline{T}}\right)\right] \tag{11}$$

Models of Table 1, modified by including the correction factor defined by Equation 9, were fitted to the rate data. Fitted parameters were b's from Equation 6, K_α from Equation 10, and K_{W1} and K_{W2} from Equation 11. Therefore, three new parameters where involved in the fitting procedure. The best modified kinetic model became:

$$r = \frac{\hat{k}_0 \cdot \left(a_P^2 - \frac{a_W a_D}{K}\right)}{a_P}\left(1 - K_W a_W^{1/\alpha}\right) \tag{12}$$

As seen in Table 1, Equation 12 corresponds to modified model I-1 (n = 1). Equation 12 stems from Mechanism 2 (ER type), by assuming adsorption of DNPE and free active sites being negligible. Equations 8 and 12 have the same driving force and include 1-pentanol in the adsorption term. The difference between both models is the role attributed to water. Equation 8 assumes a strong competitive water adsorption lessening the global reaction rate, whereas Equation 12 supposes that a part of released water remains in the catalyst blocking or inhibiting the active centers, what has a reducing effect on the global rate constant value.

Table 2 shows the values of fitted parameters of Equations 8 and 12, and their standard errors, estimated by a variation of Jackknife method[38]. As can be seen, Equation 12 yielded a better fit than Equation 8, with a decrease of the *SSR* of about 42% and, as a result, a more reliable value of the estimated reactions rate is obtained (Figure 10 down). Fitting improvement could be attributed to the fact that Equation 12 has one more parameter to fit than Equation 8, and/or that the power-type expression for water adsorption is flexible enough to properly fit rate data. Apparent activation energies of 1-pentanol dehydration to DNPE estimated from the variation of the rate constant on temperature were very similar for both models, taking into account that Jakknife method underestimates standard error. This would imply that water adsorption hardly influences the sensitivity of the reaction rate to temperature. It is to be noted that both values are similar to that obtained from experiments with no initial feed of water fitted to Equation 2 (115 ± 6 kJ/mol)[27].

Figure 12 plots the values of correction factor, $1-K_W a_W^{1/\alpha}$, as used in Equation 12 versus a_W in the whole temperature range. The correction factor decreases on increasing temperature and a_W, therefore its effect is higher. It is to be noted that trends of correction

factor and r_{DNPE} are alike for $a_W \leq 0.25$ for those experiments performed with an initial amount of water (see Figure 8). For larger a_w values, reaction rates tend to a plateau which is a function of initial water content, whereas the correction factor decreases monotonically. This could be because Freudlich isotherm is generally valid for low or intermediate species activities. On the other hand, it is expected that α decrease almost linearly with temperature, and K_w to be roughly non dependent[19,39]. Moreover α should be higher than unity. From K_α, K_{W1} and K_{W2} values it is seen that (a) α decreases with temperature, but it is lower than unity, and (b) K_W value at 463 K is nearly twice that of at 413 K. These points suggest that the fitting improvement is due to the flexibility of the power expression for θ_W and to the fact that the fitting procedure involved more parameters rather than to a fundamental insight of Freundlich isotherm. Thus, the kinetic model proposed by Equation 12 is a pseudo-empirical model rather than a mechanistic one. However, if the correction factor is considered in terms of catalyst deactivation, K_W could be considered as a deactivation constant. Consequently, from its temperature dependence a pseudo-activation energy for the water deactivation process of 24.7 ± 0.1 kJ/mol could be computed.

In Table 3, cross-correlation matrices of the fitted parameters for both Equation 8 and 12 are shown. Equation 12 presents a more desirable cross-correlation matrix, as all values other than diagonal are close to 0. In addition, as seen in Figure 11 residuals distribution for Equation 12 is nearly random, whereas, in the case of Equation 8, a clearly biased residual plot is observed.

The kinetic model proposed by Equation 8 is clearly a mechanistic one (LHHW mechanism), so it could be extrapolated to other operational conditions. On the other hand, the modified kinetic model proposed by Equation 12 (derived from a ER mechanism)

explains better the results presented in this work, but due to its pseudo-empirical background the extrapolation should be done with precaution.

4. Conclusions

Two kinetic models are proposed to explain the dehydration of 1-pentanol to DNPE in the liquid-phase. Firstly, a classical LHHW model is proposed, based on a mechanism in which the surface reaction between two adsorbed molecules of 1-pentanol is the rate-limiting step with a significant contribution of 1-pentanol and water adsorption in the denominator. On the other hand, a modified ER model is proposed, based on a mechanism in which the surface reaction between one molecule of 1-pentanol from the bulk phase and one adsorbed 1-pentanol molecule is the rate-limiting step, with a significant contribution of 1-pentanol in the denominator. The inhibiting effect of water is taken into account with a factor that modifies the actual intrinsic rate constant, in which a Freundlich-like adsorption isotherm is used. Both models fitted data satisfactorily, although the best results were obtained with the modified model. The activation energy was 118.7 ± 0.2 kJ/mol for the LHHW model and 114.0 ± 0.1 kJ/mol for the modified one. These values are very similar to the obtained when experiments with initial water and DNPE were not included in the fitting procedure.

Acknowledgements

Authors are thankful for financial support from State Education, Universities, Research & Development Office of Spain (Projects PPQ2000-0467-P4-02 and CTQ2004-01729/PPQ). Authors are also grateful to Rohm and Haas for providing the ion-exchange resin catalyst used in this work

Nomenclature

a_j activity of compound j

A, B, C, k_1	grouped factors for fitting purposes
b_i	fitted parameters
$\hat{k}$	intrinsic rate constant (mol $h^{-1}g^{-1}$)
$\hat{k}_0$	intrinsic rate constant without the effect of water (mol $h^{-1}g^{-1}$)
K_j	adsorption equilibrium constant of j
K	thermodynamic equilibrium constant
K_α, K_w	Freundlich-type correction factor constants
n	number of active sites involved in the surface reaction
n_{DNPE}	number of DNPE moles
r_{DNPE}	reaction rate of DNPE synthesis (mol $h^{-1}kg^{-1}$)
T	temperature (K)
$\overline{T}$	mean experimental temperature (K)
W	catalyst mass (g)
Greek letters	
θ_W	fraction of active centers occupied by water
Subscripts	
D	DNPE, di-n-pentyl ether
P	1-pentanol
W	water

Literature Cited

(1) Cunill, F.; Vila, M.; Izquierdo, J.F.; Iborra, M.; Tejero, J. Effect of Water Presence on Methyl *tert*-Butyl Ether and Ethyl *tert*-Butyl Ether Liquid Phase Syntheses. *Ind. Eng. Chem. Res*. **1993**, *32*, 564-569.

(2) Cruz, V.J.; Bringué, R.; Cunill, F.; Izquierdo, J.F.; Tejero, J.; Iborra, M.; Fité, C. Conversion, selectivity and kinetics of the liquid-phase dimerisation of isoamylenes in the presence of C1 to C5 alcohols catalysed by a macroporous ion-exchange resin. *J. Catal*. **2006**, *238*, 330–341.

(3) Honkela, M.; Krause, A.O.I. Kinetic modeling of the dimerization of isobutene. *Ind. Eng. Chem. Res.* **2004**, *43*, 3251-3260.

(4) Talwalkar, S.; Chauhan, M.; Aghalayam, P.; Qi, Z.; Sundmacher, K.; Mahajani, S.M. Kinetic studies on the dimerization of isobutene with ion-exchange resin in the presence of water as a selective enhancer. *Ind. Eng. Chem. Res*. **2006**, *45*, 1312-1323.

(5) Thotla, S.; Agarwal, V.; Mahajani, S.M. Aldol condensation of acetone with reactive distillation using water as a selectivity enhancer. *Ind. Eng. Chem. Res*. **2007**, *46*, 8371-8379.

(6) Jerabek, K.; Onoha, J.; Setinek, K. Kinetics of the synthesis of Bisphenol A. *Appl. Catal*. **1988**, *37*, 129-138

(7) Gates, B.; Rodriguez, W. General and specific acid catalysis in sulfonic acid resins. *J. Catal*. **1973**, *31*, 27-31.

(8) Reinicker, R.A.; Gates, B.C.; Bisphenol A Synthesis: kinetics of the phenol-acetone condensation reaction catalyzed by sulfonic acid reaction, *AIChE J*. **1974**, *20*, 933-940.

(9) Teo, H.T.R.; Saha, B. Heterogeneous catalysed esterification of acetic acid with isoamylalcohol: kinetic studies. *J. Catal*. **2004**, *228*, 174-182.

(10) Aiouache, F.; Goto, S. Sorption effect on kinetics of etherification of tert-amyl alcohol and ethanol. *Chem. Eng. Sci*. **2003**, *58*, 2065-2077.

(11) Aragon, J.M.; Vegas, J.M.R.; Jodra, L.G. Catalytic Behavior of Macroporous Resins in Catalytic Processes with water production. Activation and inhibition effects in the kinetics of the self-condensation of cyclohexanone. *Ind. Eng. Chem. Res*. **1993**, *32*, 2555-2562.

(12) Lee, M.J.; Wu, H.T.; Lin, H.M. Kinetics of catalytic esterification of acetic acid and amyl alcohol over Dowex. *Ind. Eng. Chem. Res.* **2000**, *39*, 4094-4099.

(13) Liu, W.T.; Tan, C.S. Liquid-phase esterification of propionic acid with n-butanol. *Ind. Eng. Chem. Res*. **2001**, *40*, 3281-3286.

(14) Lee, M.J.; Chiu, J.Y.; Lin, H.M. Kinetics of catalytic esterification of propionic acid and n-butanol over Amberlyst 35. *Ind. Eng. Chem. Res.* **2002**, *41*, 2882-2887.

(15) Kawase, M.; Inoue, Y.; Araki, T.; Hashimoto, K. The simulated moving-bed reactor for production of bisphenol A. *Catal. Today*. **1999**, *48*, 199-209.

(16) Podrebarac, G.G.; Ng, F.T.T.; Rempel, G.L. A kinetic study of the aldol condensation of acetone using an anion exchange resin catalyst, *Chem. Eng. Sci*. **1997**, *52* (17), 2991-3002.

(17) Yang, B.L.; Maeda, M.; Goto, S. Kinetics of Liquid Phase Synthesis of *tert*-Amyl Methyl Ether from *tert*-Amyl Alcohol and Methanol Catalyzed by Ion Exchange Resin. *Int. J. Chem. Kinet*. **1998**, *30* (2), 137-143.

(18) Limbeck, U.; Altwicker, C.; Kunz, U.; Hoffmann, U. Rate Expression for THF synthesis on acidic ion exchange resin. *Chem. Eng. Sci*. **2001**, *56*, 2171-2178.

(19) du Toit, E.; Nicol, W. The rate inhibiting effect of water as a product on reactions catalysed by cation exchange resins: formation of mesityl oxide from acetone as case study. *Appl. Catal. A: General.* **2004**, *277*, 219-225.

(20) Gates BC. *Catalytic Chemistry*. New York : Wiley, 1992, 182-253.

(21) Chakrabarti, A.; Sharma, M.M. Cationic Exchange resins as catalysts. *React. Polym*. **1993**, *20* (1-2), 1-45.

(22) Hoek, I.; Nijhuis, T.A.; Stankiewicz, A.I.; Moulijn, J.A. Kinetics of solid acid catalyzed etherification of symmetrical primary alcohols: Zeolite BEA catalyzed etherification of 1-octanol. *Appl. Catal. A: General.* **2004**, *266*, 109-116.

(23) Aiouache, F.; Goto, S. Kinetic study on 2-methyl-1-butanol dehydration catalysed by ion exchange resin. *J. Chem. Eng. Japan*. **2002**, *35*, 436-442.

(24) Sow, B.; Hamoudi, S.; Zahedi-Niaki, M.H.; Kaliaguine, S. 1-Butanol etherification over sulfonated mesostructured silica and organo-silica, *Micro. Meso. Materials.* **2005**, *79*, 129-136.

(25) Castor González, J.; Fair, J.R. Preparation of tertiary amyl alcohol in a reactive distillation column. 1. Reaction kinetics, chemical equilibrium, and mass transfer issues. *Ind. Eng. Chem Res*. **1997**, *36*, 3833-3844.

(26) Tejero, J.; Cunill, F.; Iborra, M.; Izquierdo, J.F.; Fité, C. Dehydration of 1-pentanol to di-n-pentyl ether on ion-exchange resin catalysts, *J. Mol. Cat. A: Chem*. **2002**, *182-183*, 541-554.

(27) Bringué, R.; Iborra, M.; Tejero, J.; Izquierdo, J.F.; Cunill, F.; Fite, C.; Cruz, V.J. Thermally stable ion-exchange resins as catalysts for the liquid-phase dehydration of 1-pentanol to di-n-pentyl ether (DNPE). *J. Catal*. **2006**, *244*, 33-42.

(28) Bringué, R.; Tejero, J.; Iborra, M.; Izquierdo, J.F.; Fité, C.; Cunill, F. Experimental Study of Chemical Equilibria in the Liquid-Phase Dehydration of 1-Pentanol to di-n-pentyl ether. *Ind. Eng. Chem. Res*. **2007**, *46*, 6865-6872.

(29) Bringué, R.; Tejero, J.; Iborra, M.; Izquierdo, J.F.; Fité, C.; Cunill, F. Water effect on the kinetics of 1-pentanol dehydration to di-n-pentyl ether (DNPE) on Amberlyst 70. *Top. Catal.* **2007**, *45* (1-4), 181-186.

(30) Medina, E. MS Chemical Engineering Thesis. University of Barcelona. 2007

(31) Wittig, R.; Lohmann, J.; Gmehling, J. Vapor-Liquid Equilibria by UNIFAC Group Contribution. 6. Revision and Extension. *Ind. Eng. Chem. Res*. **2003**, *42*, 183-188.

(32) Tejero, J.; Cunill, F.; Izquierdo, J.F. Vapor-Phase Addition of Methanol to Isobutene on a Macroporous Resin. A Kinetic Study. *Ind. Eng. Chem. Res.* **1989**, *28*, 1269-1277.

(33) Iborra, M.; Izquierdo, J.F.; Cunill, F.; Tejero, J**.** Application of the Response Surface Methodology to the Kinetic Study of the Gas-Phase Addition of Ethanol to Isobutene on a Sulfonated Styrene-Divinylbenzene Resin. *Ind. Eng. Chem. Res*. **1992**, *31*, 1840-1848.

(34) Cunill, F.; Tejero, J.; Fité, C.; Iborra, M.; Izquierdo, J.F. Conversion, Selectivity, and Kinetics of the Dehydration of 1-Pentanol to di-n-Pentyl ether Catalyzed by a Microporous Ion-Exchange Resin. *Ind. Eng. Chem. Res*. **2005**, *44*, 318-324.

(35) Tejero, J.; Cunill, F.; Iborra, M.; Izquierdo, J.F.; Fité, C.; Bringué, R. Liquid-phase dehydration of 1-pentanol to di-n-pentyl ether (DNPE) over medium and large pore acidic zeolites. *Micro. Meso. Materials* **2009**, *117* (3), 650-660.

(36) Iborra, M.; Tejero, J.; Cunill, F.; Izquierdo, J.F.; Fité, C. Drying of Acidic Macroporous Styrene-Divinylbenzene Resins with 12-20% Crosslinking Degree. *Ind. Eng. Chem. Res*. **2000**, *39* (5), 1416-1422.

(37). Ancillotti, F.; Massi Mauri, M.; Pescarollo, E. Ion exchange-resin catalysed addition of alcohol to olefins. *J. Catal*. **1977**, *46*, 49-57.

(38) Caceci, M.S. Estimating error limits in parametric curve fitting**.** *Anal. Chem*. **1989**, *61*, 2324-2327.

(39) Adamson, A.W. *Physical Chemistry of Surface*, Fifth Edition Wiley, New York. 1990, 421-426

Figures

Figure 1. Effect of resin particle size on DNPE production (up) and the initial reaction rate (down) at 463K, N = 500 rpm, 1g dry Amberlyst 70.

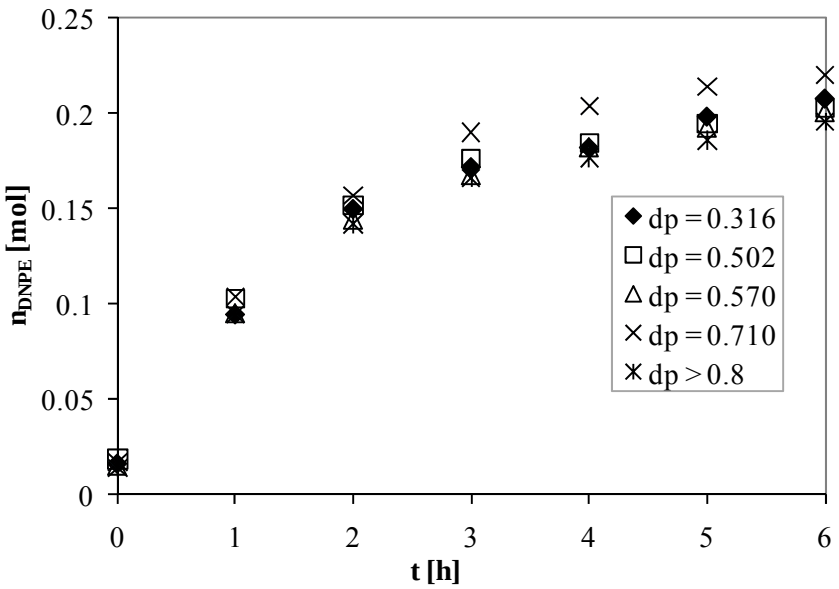

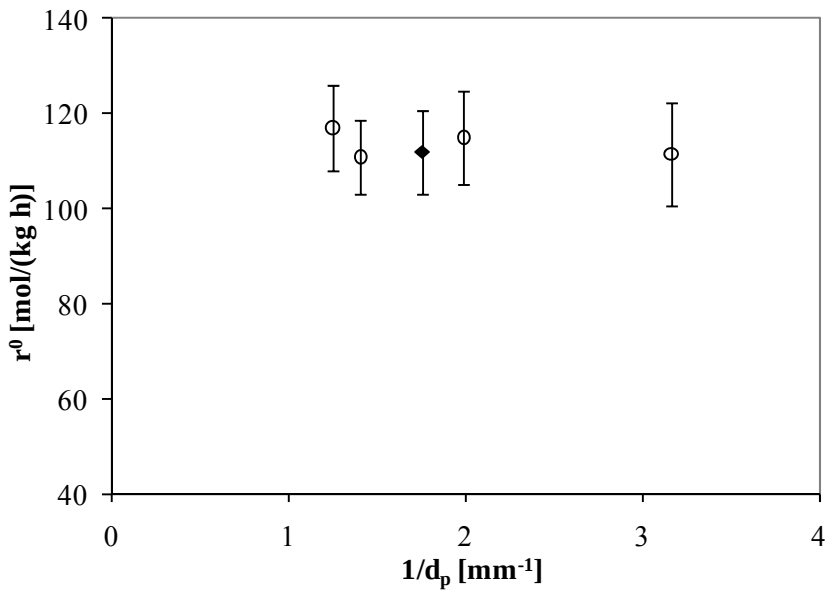

510 Figure 2. Effect of stirring speed on DNPE production (up) and the initial reaction rate

511 (down) at 463K, 1g of dried commercial beads of Amberlyst 70.

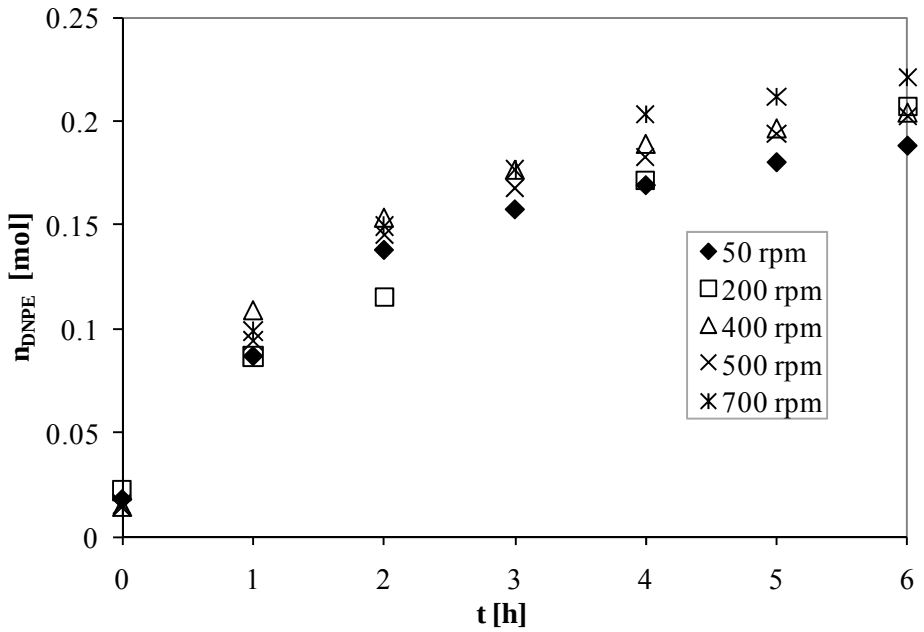

512

513

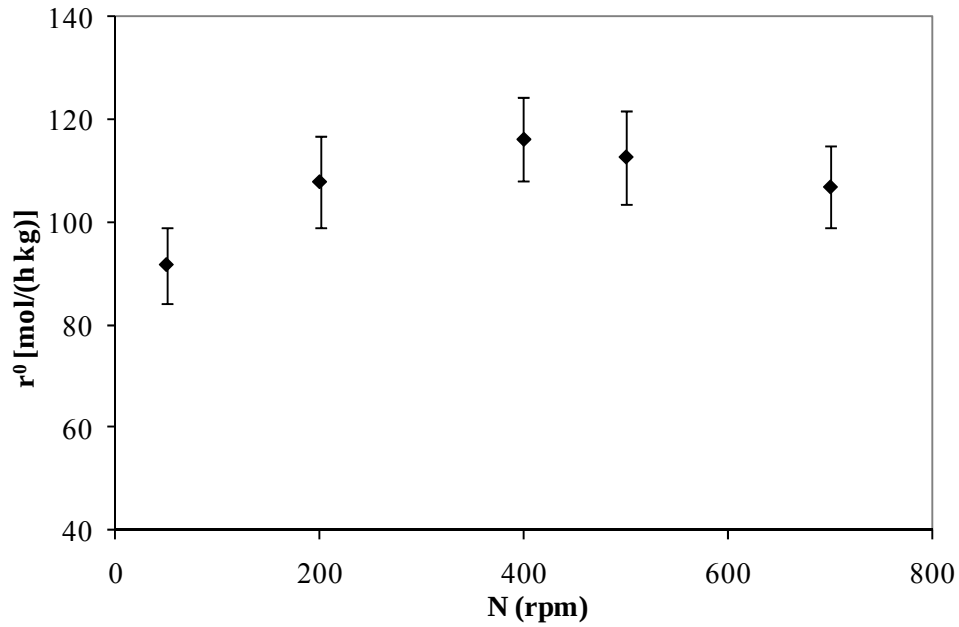

514

515

516 Figure 3. DNPE mole profile versus time at temperatures tested.

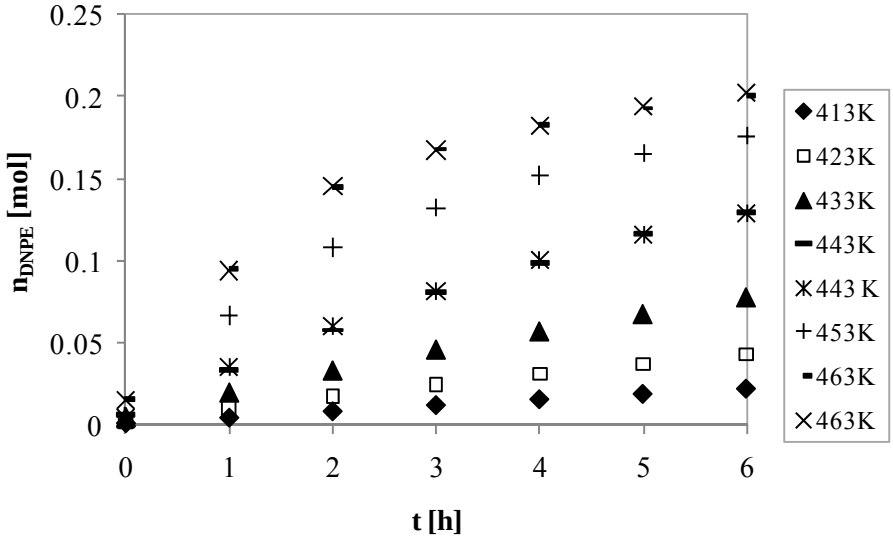

517

518

519 Figure 4. Reaction rate of DNPE synthesis as a function of 1-pentanol (up), DNPE

520 (middle) and water (down) activities in the temperature range explored

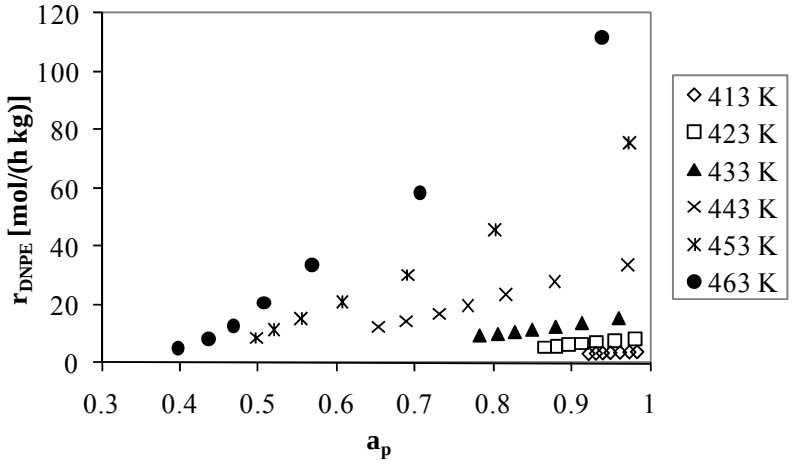

521

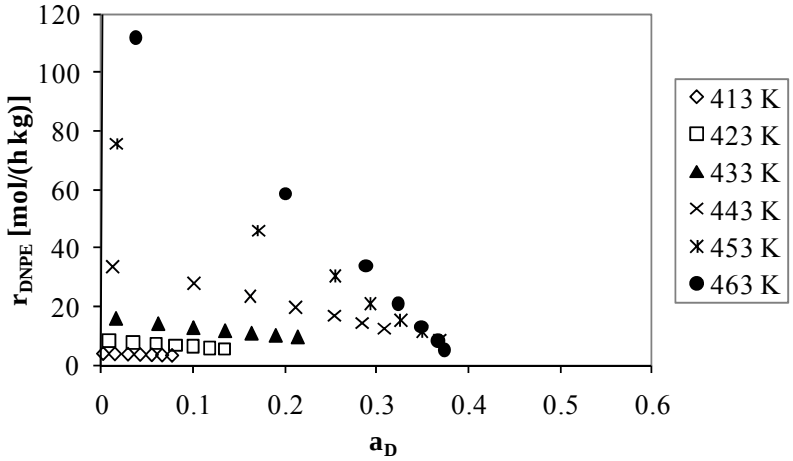

522

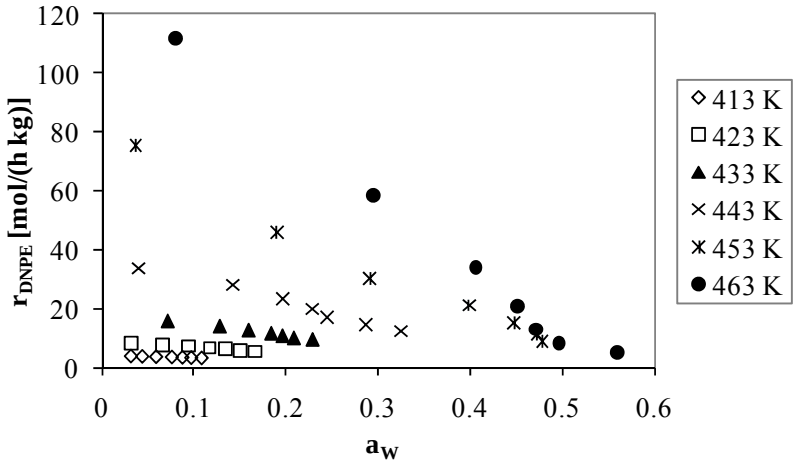
120
100
80
60
40
20
0
0
0.1
0.2
0.3
0.4
0.5
0.6
r_{DNPE} [mol/(h kg)]
a_W
413 K
423 K
433 K
443 K
453 K
463 K

523

524

Figure 5. Comparison of the goodness of fit in terms of SSR_{min}/SSR.

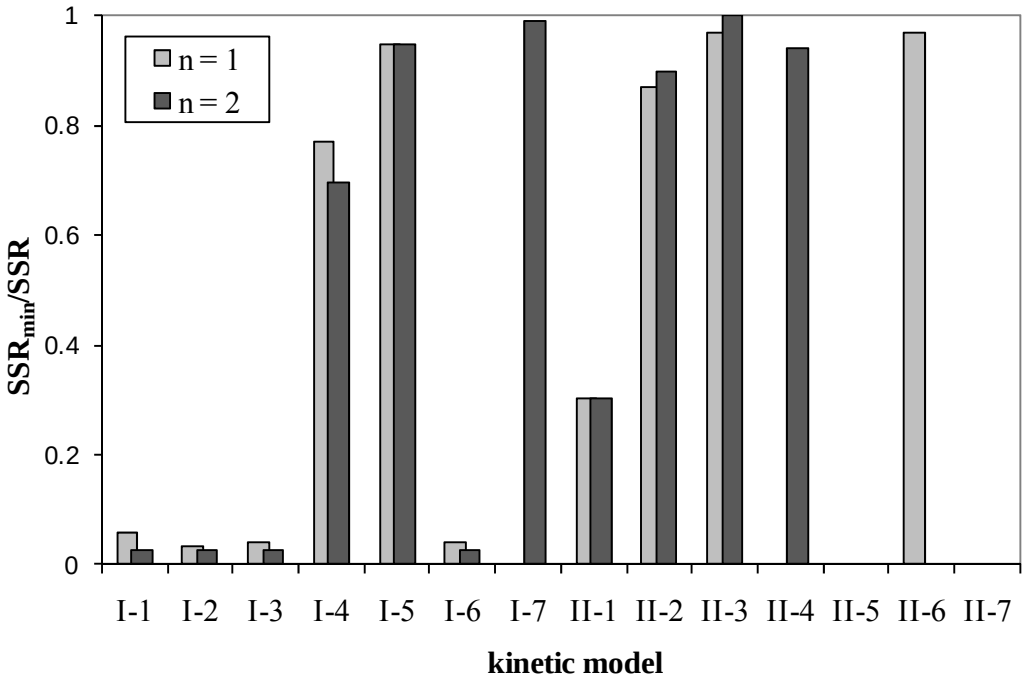

Figure 6. Particle size distribution in dry air, 1-pentanol, DNPE and water for Amberlyst 70.

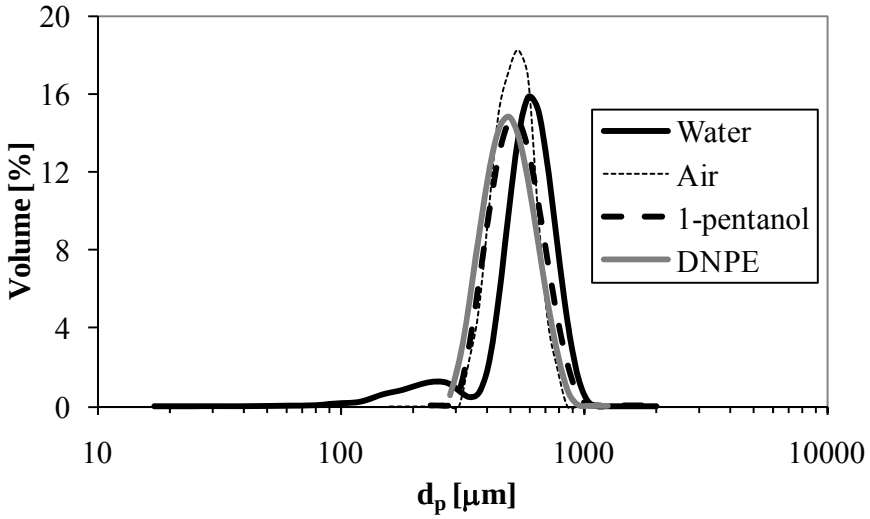

Figure 7. DNPE mole profile versus time for different initial amounts of water (up) and DNPE (down) in the initial mixture at 433K

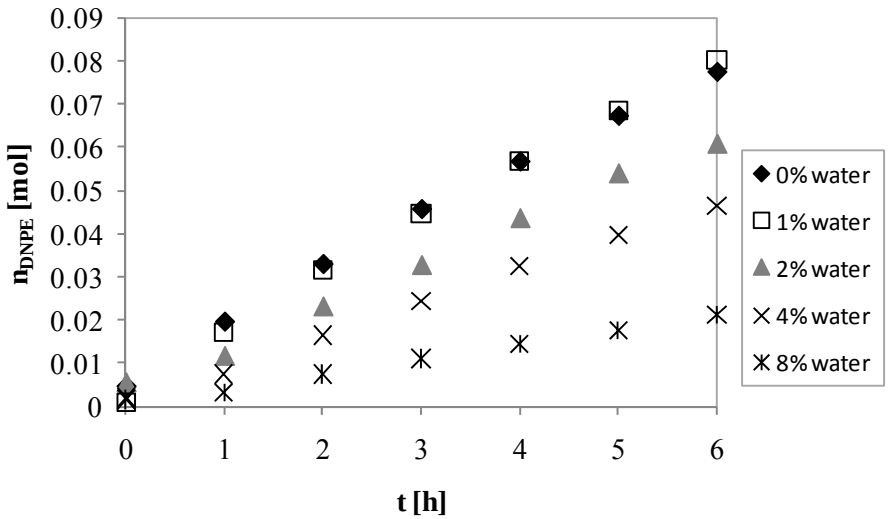

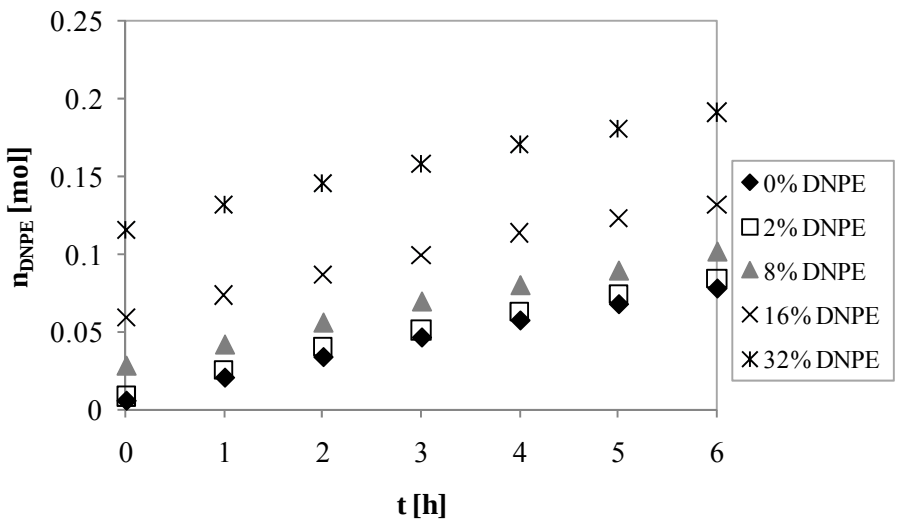

Figure 8. Effect of DNPE (up) and water (down) activities on the reaction rate at 433K at different initial mixtures 1-pentanol/water and 1-pentanol/DNPE (Dotted lines join initial reaction rate data)

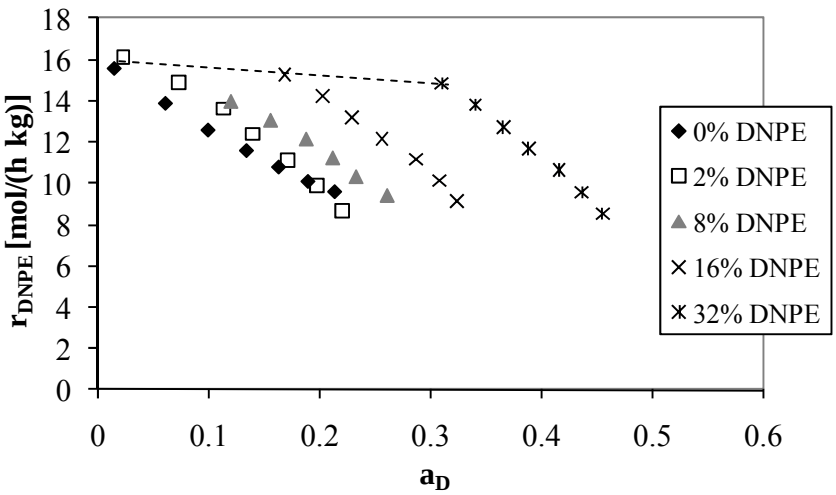

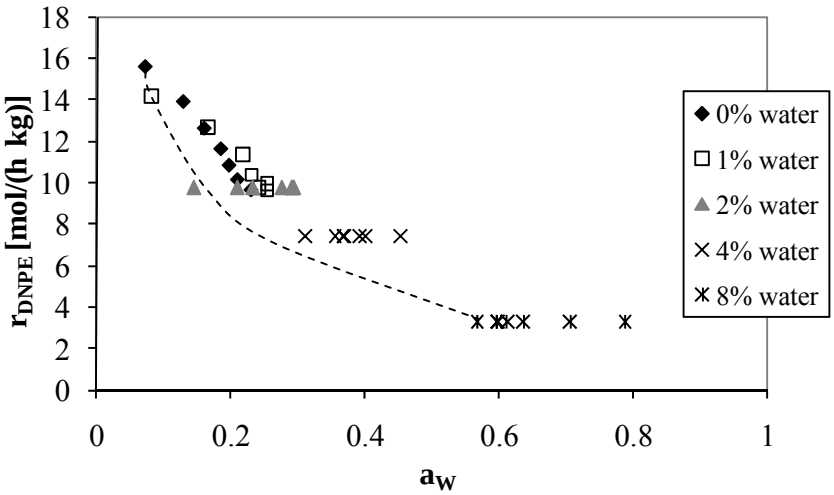

Figure 9. Comparison of goodness of fit in terms of SSR_{min}/SSR when including experiments with initial amounts of water and DNPE.

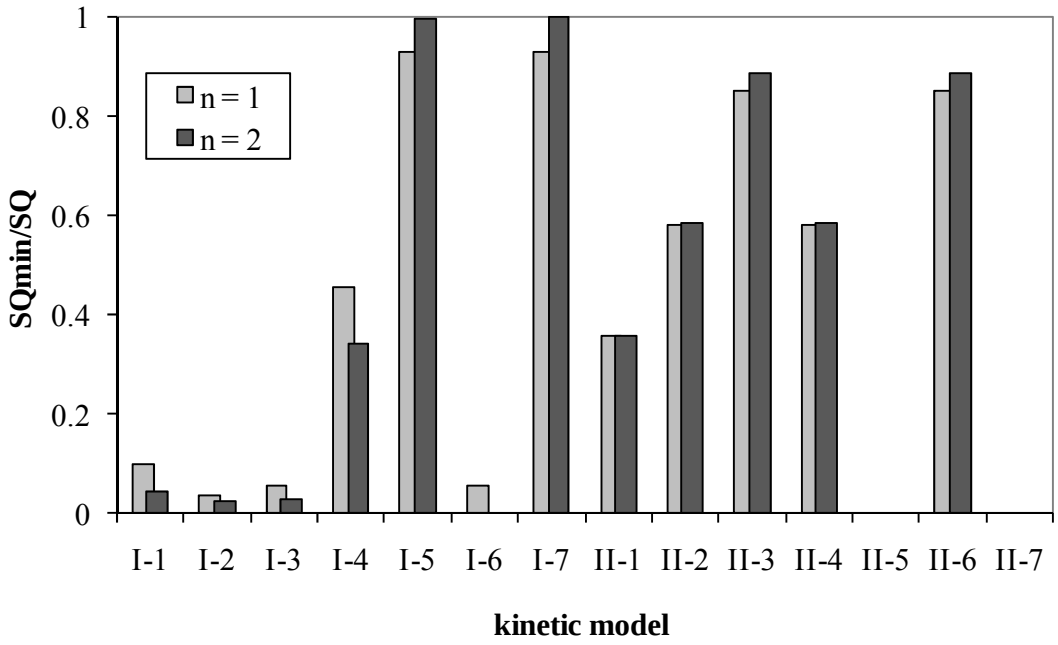

Figure 10. Calculated reaction rates by Equation 8 (up) and by Equation 12 (down) versus experimental rates in the whole temperature range

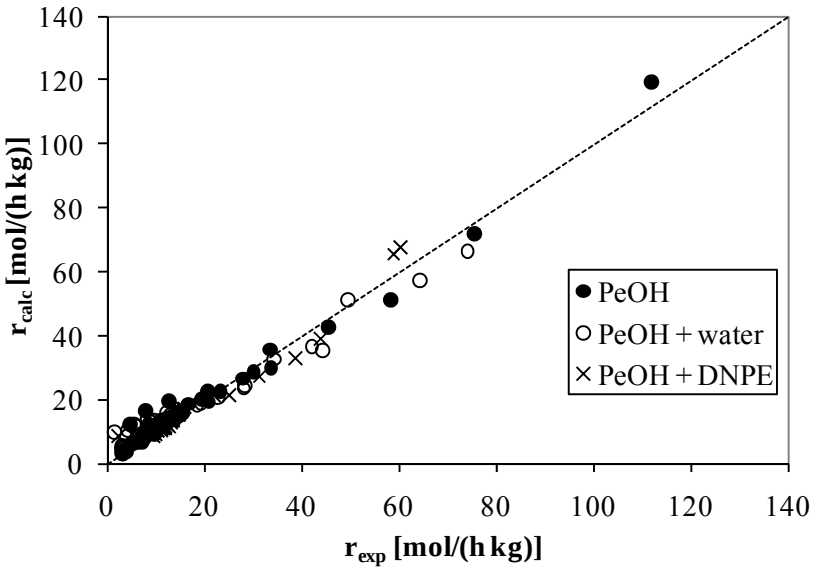

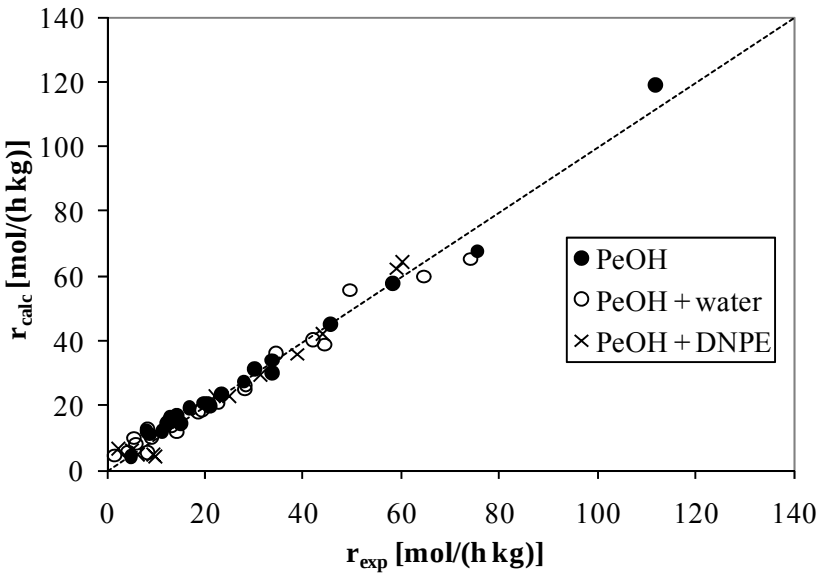

Figure 11. Residuals distribution for Equation 8 (up) and Equation 12 (down).

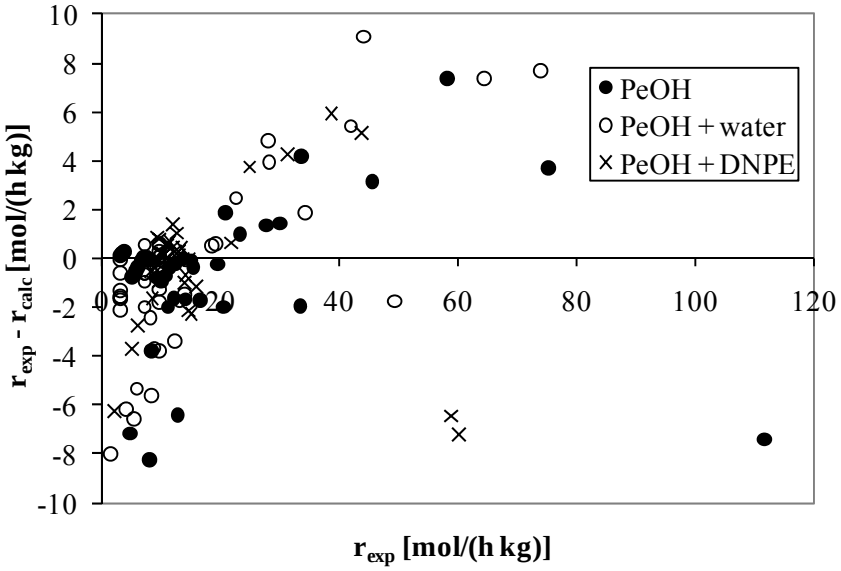

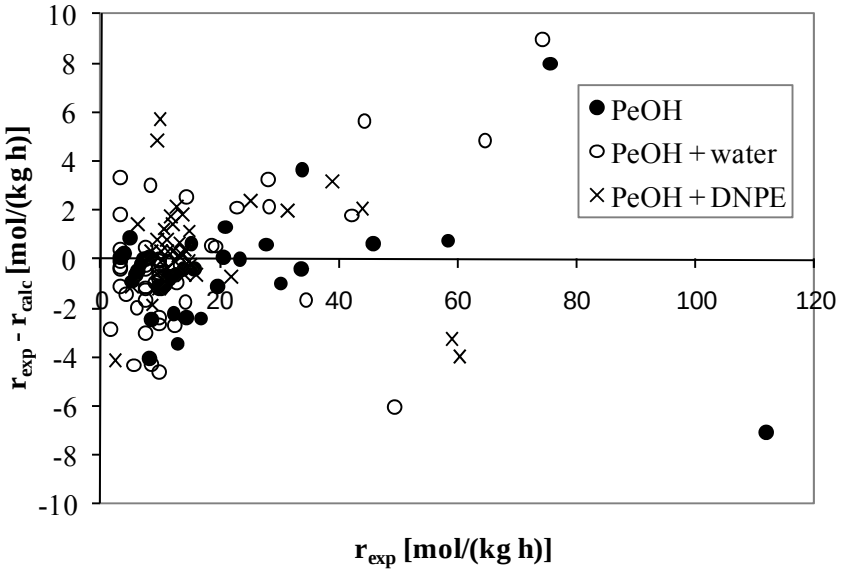

Figure 12. Computed correction factor versus a_w in the whole temperature range

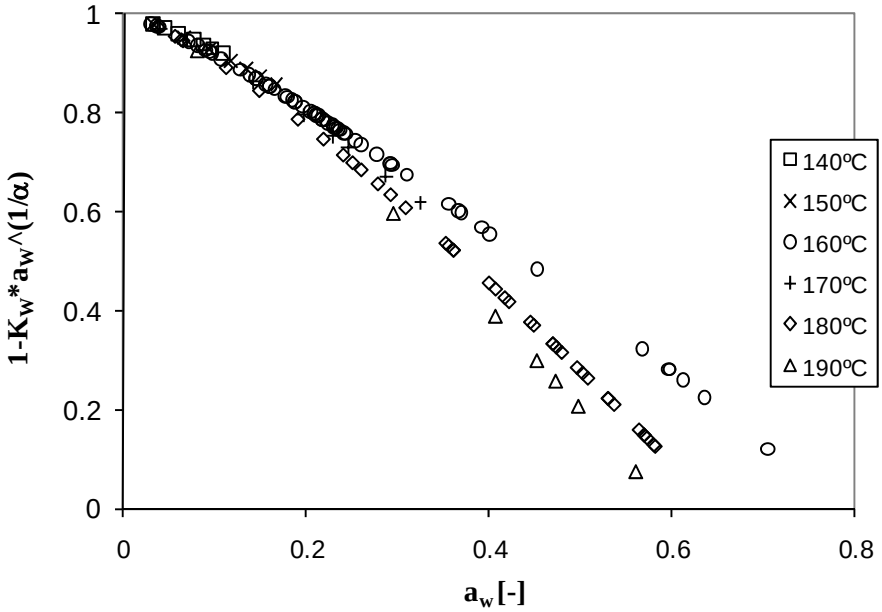

Tables

Table 1. Kinetic models tested with *n* values ranging from 1 to 2

TYPE	CLASS I	CLASS II
1	$r = A\dfrac{\left(a_P^2 - \dfrac{a_D a_W}{K}\right)}{a_P^n}$	$r = \dfrac{k_1\left(a_P^2 - \dfrac{a_D a_W}{K}\right)}{\left(1 + K_P\, a_P\right)^n}$
2	$r = A\dfrac{\left(a_P^2 - \dfrac{a_D a_W}{K}\right)}{a_D^n}$	$r = \dfrac{k_1\left(a_P^2 - \dfrac{a_D a_W}{K}\right)}{\left(1 + K_D\, a_D\right)^n}$
3	$r = A\dfrac{\left(a_P^2 - \dfrac{a_D a_W}{K}\right)}{a_W^n}$	$r = \dfrac{k_1\left(a_P^2 - \dfrac{a_D a_W}{K}\right)}{\left(1 + K_W\, a_W\right)^n}$
4	$r = \dfrac{A\left(a_P^2 - \dfrac{a_D a_W}{K}\right)}{\left(a_P + B\, a_D\right)^n}$	$r = \dfrac{k_1\left(a_P^2 - \dfrac{a_D a_W}{K}\right)}{\left(1 + K_P\, a_P + K_D\, a_D\right)^n}$
5	$r = \dfrac{A\left(a_P^2 - \dfrac{a_D a_W}{K}\right)}{\left(a_P + B\, a_W\right)^n}$	$r = \dfrac{k_1\left(a_P^2 - \dfrac{a_D a_W}{K}\right)}{\left(1 + K_P\, a_P + K_W\, a_W\right)^n}$
6	$r = \dfrac{A\left(a_P^2 - \dfrac{a_D a_W}{K}\right)}{\left(a_D + B\, a_W\right)^n}$	$r = \dfrac{k_1\left(a_P^2 - \dfrac{a_D a_W}{K}\right)}{\left(1 + K_D\, a_D + K_W\, a_W\right)^n}$
7	$r = \dfrac{A\left(a_P^2 - \dfrac{a_D a_W}{K}\right)}{\left(a_P + B\, a_D + C\, a_W\right)^2}$	$r = \dfrac{k_1\left(a_P^2 - \dfrac{a_D a_W}{K}\right)}{\left(1 + K_P\, a_P + K_D\, a_D + K_W\, a_W\right)^2}$

Table 2. Parameters of the fitting procedure of Equations 8 (b_1 and b_2 corresponding to A and b_3 and b_4 to B, according to Equation 6) and 12 (b_1 and b_2 corresponding to $\hat{k}_0$)

	Equation 8	Equation 12
b_1	2.160 ± 0.003	2.122 ± 0.002
b_2	14275 ± 25	13710 ± 15
b_3	0.007 ± 0.006	
b_4	2952 ± 38	
K_{w1}		495 ± 4
K_{w2}		2971 ± 49
K_α		358 ± 1
E_a (kJ/mol)	118.7 ± 0.2	114.0 ± 0.1
SSR	1190	690
SSR variation over Equation 8 (%)	0	-42

Table 3. Correlation matrix of fitted parameters for Equation 8 (b_i are the fitting parameters of factors A and B of the model) and Equation12 (b_i and K_{Wi} are the fitting parameters of factors A and K_W of the model), respectively.

Equation 8				
	b_1	b_2	b_3	b_4
b_1	1			
b_2	-0.97	1		
b_3	0.85	-0.78	1	
b_4	-0.88	-0.84	-0.97	1

Equation 12					
	b_1	b_2	K_{W1}	K_{W2}	K_α
b_1	1				
b_2	-0.04	1			
K_{W1}	0.03	-0.06	1		
K_{W2}	0.13	-0.07	0.32	1	
K_α	0.10	0.00	-0.22	0.05	1